JCB Report

Dynein/dynactin regulate metaphase spindle length by targeting depolymerizing activities to spindle poles

Jedidiah Gaetz and Tarun M. Kapoor

Laboratory of Chemistry and Cell Biology, The Rockefeller University, New York, NY 10021

During cell division metaphase spindles maintain constant length, whereas spindle microtubules continuously flux polewards, requiring addition of tubulin subunits at microtubule plus-ends, polewards translocation of the microtubule lattice, and removal of tubulin subunits from microtubule minus-ends near spindle poles. How these processes are coordinated is unknown. Here, we show that dynein/dynactin, a multi-subunit microtubule minus-end–directed motor complex, and NuMA, a microtubule cross-linker, regulate spindle length. Fluorescent speckle microscopy reveals that dynactin or NuMA inhibition suppresses microtubule disassembly at spindle poles without affecting polewards microtubule sliding. The observed uncoupling of these two components of flux indicates that microtubule depolymerization is not required for the microtubule transport associated with polewards flux. Inhibition of Kif2a, a KinI kinesin known to depolymerize microtubules in vitro, results in increased spindle microtubule length. We find that dynein/dynactin contribute to the targeting of Kif2a to spindle poles, suggesting a model in which dynein/dynactin regulate spindle length and coordinate flux by maintaining microtubule depolymerizing activities at spindle poles.

Introduction

During mitosis, a bipolar spindle is assembled to accurately segregate the replicated DNA into two daughter cells. The shape and size of the spindle determine the distance over which DNA is segregated and impact the forces acting on chromosomes. Spindle organization depends on microtubules, polymers of tubulin. Spindle microtubules have been shown to undergo a process referred to as polewards flux (Mitchison, 1989; Maddox et al., 2002; Rogers et al., 2004). At metaphase, this involves the continuous addition of tubulin subunits to microtubule plus-ends, polewards translocation of microtubules, and microtubule disassembly at spindle poles. Surprisingly, all of these events are coordinated so that spindle length and average spindle microtubule length remain unchanged whereas microtubules flux polewards. Recent studies have shown that microtubule polymerization and transport can each be regulated by microtubule-associated proteins (for reviews see Cassimeris, 1999; Wittmann et al., 2001). These include motor proteins, such as Eg5 and dynein, that can slide microtubules, as well as kinesins in the KinI family and nonmotor proteins that can regulate microtubule polymerization. It is not known how activities of these proteins are regulated at different sites within spindles to maintain steady-state length.

During polewards flux, microtubule disassembly occurs at spindle poles, whereas microtubule ends remain focused. Dynein and dynactin are large (>1 MD) multi-subunit complexes that localize to spindle poles (for review see Karki and Holzbaur, 1999). Recent studies suggest that a complex of dynein and dynactin plays an important role in transporting and targeting a number of proteins to spindle poles (for example, Mad2; Howell et al., 2001). NuMA, a microtubule cross-linking protein that plays a key role in spindle pole formation, is transported to spindle poles, most likely through interactions with dynein/dynactin (Gaglio et al., 1995; Merdes et al., 1996). Additionally, dynein contributes to the polewards transport of short stabilized exogenous microtubules added to spindles (Heald et al., 1996). These data suggest that dynein and dynactin may also drive the translocation of spindle microtubules during polewards flux. However, this possibility has not been directly tested. Here, we show that dynein, dynactin, and their binding partner NuMA, can control spindle microtubule length by contributing to the targeting of the depolymerizing activities of a KinI kinesin to spindle poles without directly affecting the translocation of microtubules associated with polewards flux.

The online version of this article contains supplemental material.

Address correspondence to Tarun M. Kapoor, Lab of Chemistry and Cell Biology, The Rockefeller University, 1230 York Ave., Box 202, New York, NY 10021. Tel.: (212) 327-8176. Fax: (212) 327-8177. email: kapoor@rockefeller.edu

Key words: microtubule; kinesin; spindle; mitosis; dynactin

© The Rockefeller University Press, 0021-9525/2004/08/465/7 $8.00
The Journal of Cell Biology, Volume 166, Number 4, August 16, 2004 465–471
http://www.jcb.org/cgi/doi/10.1083/jcb.200404015

The Journal of Cell Biology

Results and discussion

Inhibition of dynein and dynactin results in the elongation of spindle microtubules

To examine the role of dynactin in polewards flux in bipolar spindles, we used an inhibitor named p150-CC1. This recombinant protein fragment consists of amino acids 217–548 of the $p150^{Glued}$ subunit of dynactin and has been shown to bind dynein in vitro and inhibit dynactin function (Quintyne et al., 1999; King et al., 2003). For these experiments we used spindles assembled in *Xenopus* egg extracts (Desai et al., 1999a). An advantage of this cell-free system is that spindles are not constrained in fixed volumes and cell cortices are absent, allowing mechanisms intrinsic to the spindle to be examined.

p150-CC1 was added to spindles assembled in egg extracts cycled through interphase to replicate their DNA and centrosomes. Individual spindles were monitored by time-lapse microscopy. Within ~7 min of p150-CC1 (2 μM) addition, spindle length doubled while bipolar organization was maintained (Fig. 1, D–G). Measurements revealed that the distance between opposite poles increased at 4.5 ± 0.9 μm/min (12 live recordings, two independent experiments) after p150-CC1 treatment, whereas control spindles did not change length (Fig. 1, A–C; Videos 1 and 2, available at http://www.jcb.org/cgi/content/full/jcb.200404015/DC1). Microtubule focusing at poles was not significantly perturbed in p150-CC1–treated spindles that were twice as long as untreated spindles (Fig. 1, H, I, and O). At >25 min after p150-CC1 addition, structures were often longer than 3.5 times the length of control spindles (~140 μm; unpublished data). Analysis of fixed samples revealed that the effect of p150-CC1 on spindle length increase was dose dependent, and the effect saturated by 2 μM (IC_{50} = ~300 nM; Fig. 1 J). These data demonstrate that dynactin is required for maintaining constant spindle length.

To examine whether the effect of p150-CC1 on spindle length was due to inhibition of the activity of the dynein/dynactin complex, we tested the effect of available dynein inhibitors, the antibody 70.1 and vanadate. Spindles treated with 70.1 (1 mg/ml; note: ~800 nM dynein in egg extracts), an antibody to dynein intermediate chain, increased in length at 3.7 ± 0.9 μm/min (42 spindles, two independent experiments; Fig. 1 M). Similar effects were observed for vanadate-treated (100 μM) spindles (Fig. S1, available at http://www.jcb.org/cgi/content/full/jcb.200404015/DC1). These data are consistent with both dynein motor activity and dynactin regulating spindle length.

We find p150-CC1 to be significantly more potent than the commonly used dynactin inhibitor p50 dynamitin (Echeverri et al., 1996; Wittmann and Hyman, 1999). No effect on assembled spindles was observed at 18 μM p50 dynamitin, the maximum concentration that we could use without perturbing extracts by dilution alone. However, as previously reported, p50 dynamitin (18 μM) added at the start of spindle assembly resulted in structures with unfocused poles and lengths within 20% of that of untreated spindles (Fig. S1). Addition of 2 μM p150-CC1 at the start of spindle assembly resulted in very long spindles similar to that shown

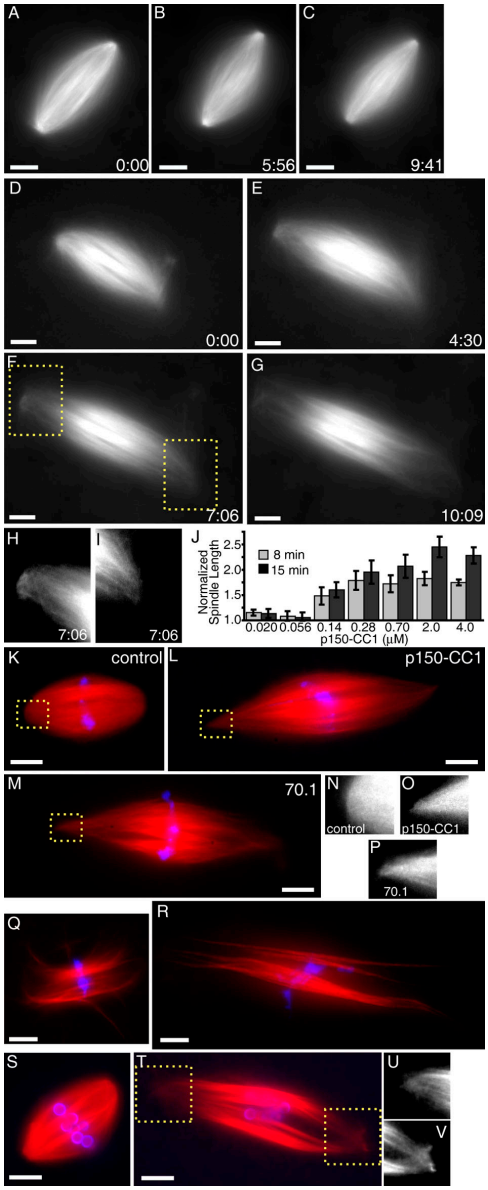

Figure 1. **Dynein/dynactin inhibition increases the length of spindle microtubules in the presence or absence of centrosomes.** (A–C) Tubulin distribution in untreated spindles during live recordings. (D–G) p150-CC1 addition (2 μM, ~3 min before image at t = 0) caused spindles to increase in length. (H and I) Higher magnified spindle pole regions indicated in F (Videos 1 and 2). (J) p150-CC1 was added to assembled spindles, samples were fixed after 8 or 15 min, spindle lengths were measured (mean ± SD, *n* = 15, two independent experiments), and normalized to the length of untreated spindles (40 μm). (K–M) Spindles fixed 8 min after addition of control buffer (K), 2 μM p150-CC1 (L), or 1 mg/ml 70.1 (M) (tubulin, red; DNA, blue). (N–P) Higher magnified, contrast-adjusted regions indicated in K–M, respectively. (Q and R) Spindles assembled in 18 μm p50 dynamitin were treated with control buffer (Q) or 2 μm p150-CC1 (R) and fixed after 15 min (tubulin, red; DNA, blue). (S and T) Spindles assembled in the absence of centrosomes, around DNA-beads (tubulin, red; DNA, blue). (S) Buffer control. (T) p150-CC1–treated (2 μM, 8 min). (U and V) Higher magnified, contrast-adjusted regions indicated in R. Times are in min:s. Bars, 10 μm.

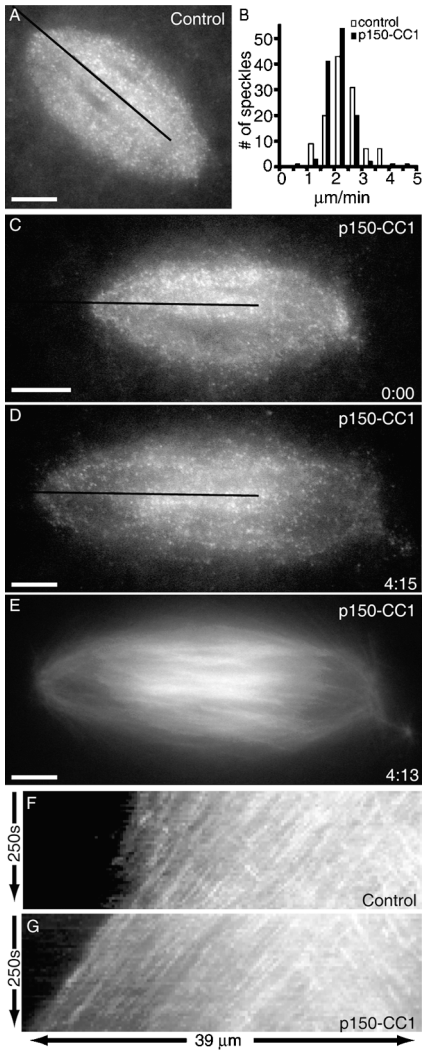

Figure 2. **Dynactin inhibition with p150-CC1 suppresses microtubule depolymerization at spindle poles.** Spindle microtubule dynamics were analyzed using fluorescent speckle microscopy. (A) Tubulin speckles in a control spindle. (B) Polewards velocities of tubulin speckles in control (white bars; 2.1 ± 0.3 μm/min, mean ± SD), or p150-CC1–treated (2 μM p150-CC1, black bars; 2.1± 0.2 μm/min, mean ± SD) spindles (n = 12 for each condition, 120 speckles). Velocities were binned in 0.5 μm/min increments. (C–E) Images from a time-lapse video of a p150-CC1–treated spindle (2 μM p150-CC1 added ~3 min before image at t = 0) showing tubulin speckles (C and D) and tubulin distribution (E). The black lines in A, C, and D indicate the regions used to generate the kymographs shown in F and G, respectively (Videos 3 and 4). Times are in min:s. Bars, 10 μm.

in Fig. 1 G. An effect similar to that of p50 dynamitin was observed with low concentrations p150-CC1 (56 nM), if added at the start of spindle assembly. It is possible that differences in p50 dynamitin and p150-CC1 potencies reflect their different mechanisms of inhibiting dynactin function. It noteworthy that addition of p150-CC1 (to 2 μM) to spindles with unfocused poles, that were assembled in the presence of high concentration of p50 dynamitin or low concentrations of p150-CC1, resulted in spindle elongation at the same rate as spindles treated with p150-CC1 alone (2 μM; Fig. 1, Q and R; Fig. S1). These data indicate that the role of dynactin in spindle microtubule length regulation is independent of its function in pole focusing.

Dynein and dynactin associate with centrosomes and play a role in tethering centrosomes to spindle microtubules (Heald et al., 1997; Quintyne et al., 1999). To examine whether the spindle elongation observed upon dynein or dynactin inhibition depended on centrosome function, we tested the effect of p150-CC1 addition to spindles assembled in the absence of centrosomes. DNA-coated beads, when added to *Xenopus* egg extracts, induce the assembly of centrosome-free spindles morphologically indistinguishable from spindles assembled around sperm chromatin (Heald et al., 1996). Analysis of fixed samples (Fig. 1, S–V), as well as real-time analysis (not depicted), revealed that inhibition of dynactin with p150-CC1 resulted in the elongation of centrosome-free spindles. In the presence of p150-CC1 (2 μM), spindles elongated at 3.1 ± 0.2 μm/min (average of 26 spindles, two independent experiments). Similar results were obtained when antibody 70.1 was added to DNA-bead spindles (unpublished data). These data are consistent with a role for dynein and dynactin in maintaining the length of spindle microtubules independent of their function at centrosomes.

Inhibition of dynactin in bipolar spindles suppresses disassembly of microtubules at spindle poles

Dynein/dynactin inhibition could, in principle, increase spindle microtubule length by affecting the polewards transport of microtubules or by suppressing disassembly at spindle poles. To distinguish between these possibilities, we used fluorescent speckle microscopy (Waterman-Storer et al., 1998) to analyze microtubule dynamics in spindles treated with p150-CC1, the dynactin inhibitor for which we had determined dose-dependence and saturating concentrations. To track microtubule organization in time-evolving structures we used multi-wavelength fluorescence microscopy, recording fluorescent speckles, overall microtubule organization, and as needed, the position of DNA (Fig. 2). Rates of tubulin translocation were measured by kymography and confirmed by manual tracking of individual speckles (Fig. 2, B, F, and G).

Fig. 2 (A and F) show polewards flux in an untreated spindle (Video 3, available at http://www.jcb.org/cgi/content/full/jcb.200404015/DC1). Analysis revealed that tubulin speckles moved toward the spindle pole at 2.4 ± 0.7 μm/min (Fig. 2, B and F). In p150-CC1 treated spindles (Fig. 2, C–E) the rate of polewards microtubule sliding, was 2.1 ± 0.4 μm/min, indistinguishable from that in untreated spindles (Fig. 2, B and G). The speckles did not move relative to the spindle pole, but moved along with the pole at half the speed the poles moved apart (elongation rate = 4.5 ± 0.9 μm/min; Fig. 2 G; Video 4, available at http://www.jcb.org/cgi/content/full/jcb.200404015/DC1). Analysis of fluorescent speckle microscopy data also revealed that there was not a significant difference in the size of the region of bidirectional speckle movement in untreated and p150-CC1–treated spindles, suggesting that dynactin inhibition did not affect the extent of antiparallel microtubule overlap in the spindle (Fig. 2, F and G).

These data indicate that the spindle elongation observed upon inhibition of dynactin with p150-CC1 is due to a lack of microtubule minus-end disassembly at spindle poles, and that this occurs without any significant perturbation of poleward microtubule sliding in the spindle.

NuMA inhibition results in elongation of spindle microtubules

NuMA has been shown to interact with dynein/dynactin, and NuMA targeting to spindle poles depends on dynactin function (Merdes et al., 2000). Consistent with these data, we found that p150-CC1 treatment disrupted NuMA targeting to spindle poles (Fig. S2, available at http://www.jcb.org/cgi/content/full/jcb.200404015/DC1). To examine whether NuMA cooperates with dynein and dynactin in regulating the length of spindle microtubules, we perturbed NuMA function in spindles using the NuMA-binding domain of LGN, a mammalian Pins homologue (Yu et al., 2000; Du et al., 2001, 2002). This recombinant protein fragment, consisting of amino acids 1–373 of LGN (hereafter named LGN-N), inhibits NuMA interactions with microtubules both in vitro and in vivo (Du et al., 2001, 2002).

Addition of LGN-N to spindles assembled in *Xenopus* extracts had an effect similar to that of perturbing dynein or dynactin (Fig. 3, A–E; Video 5, available at http://www.jcb.org/cgi/content/full/jcb.200404015/DC1). Real-time analysis of individual spindles and measurements of fixed samples revealed that spindles treated with LGN-N increased in length while maintaining bipolar organization. At 4 μM LGN-N spindle length increased at 4.3 ± 0.6 μm/min (n = 26 spindles, two independent experiments). At these concentrations of LGN-N (compared with ~50 nM NuMA in *Xenopus* egg extracts; Merdes et al., 1996), NuMA was displaced from spindle poles (Fig. S2). Fluorescent speckle microscopy revealed that the poleward sliding rate of microtubules in the spindle was not perturbed by LGN-N treatment (2.3± 0.7 μm/min; unpublished data) relative to control spindles (2.4 ± 0.7 μm/min; Fig. 2 B). Recombinant LGN, fused to either GST, or to a polyhistidine tag, gave similar results in these experiments. As with dynein or dynactin inhibition, the length of centrosome-free spindles assembled around DNA beads also increased upon LGN-N treatment (Fig. 3, F–H).

These data demonstrate that NuMA cooperates with dynein/dynactin to regulate microtubule minus-end dynamics at spindle poles without directly contributing to the sliding component of polewards flux.

Kif2a plays a key role in spindle assembly and maintenance

We considered the possibility that dynein, dynactin, and NuMA may regulate spindle microtubule length by targeting microtubule-depolymerizing activities to spindle poles. Two vertebrate kinesins in the KinI family, Kif2a and MCAK/XKCM1/Kif2c (hereafter referred to as MCAK), have been shown to have microtubule depolymerizing activities in vitro (Desai et al., 1999b). The function of MCAK during spindle assembly in the *Xenopus* extract system has been extensively studied (Walczak et al., 1996, 2002). Although a functional role for Kif2a has been described in neurons (Noda et al., 1995), a role in spindle assembly has not been shown.

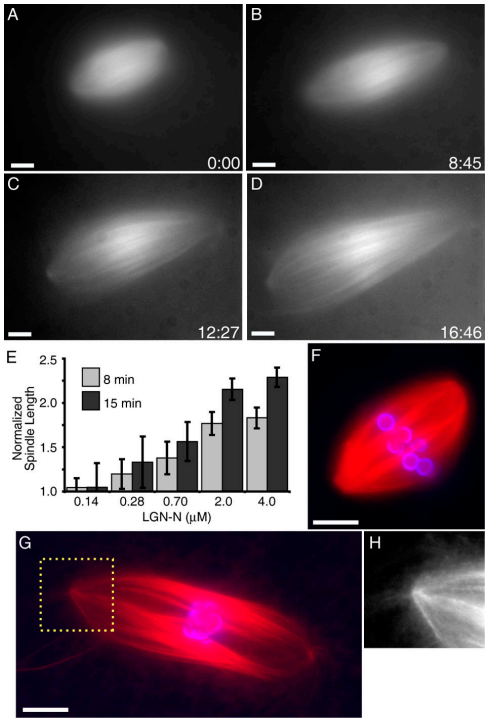

Figure 3. **NuMA inhibition with LGN-N increases the length of spindle microtubules, in the presence or absence of centrosomes.** (A–D) Tubulin distribution in an LGN-N–treated spindle (0.7 μM, added ~3 min before image at t = 0) during live recordings (Video 5). (E) LGN-N was added to assembled spindles, samples were fixed after 8 or 15 min, spindle lengths were measured (mean ± SD, n = 15, two independent experiments), and normalized to the length of untreated spindles (40 μm). (F–H) Spindles assembled in the absence of centrosomes, around DNA beads (tubulin, red; DNA, blue). (F) Buffer control. (G) LGN-N–treated (2 μM, 8 min). (H) Higher magnified image of the region indicated in G. Times are in min:s. Bars, 10 μm.

To examine Kif2a function in spindles, we used a polyclonal antibody raised against the NH_2 terminus of Kif2a to block its function. Similar antibodies, raised against the NH_2 terminus of the closely related KinI MCAK have been shown to block MCAK microtubule destabilizing activity (Walczak et al., 1996). In Western blots, the Kif2a antibody was found to be mono-specific, recognizing a ~100-kD band, which is consistent with the predicted size of *Xenopus* Kif2a (Fig. 4 A). Addition of Kif2a antibody (0.7 mg/ml) at the start of spindle assembly, after DNA and centrosome replication, resulted in the formation of large monopolar structures with unusually long extended microtubule bundles (Fig. 4, B and C). These results are similar to those observed in mammalian cells after suppression of Kif2a protein levels using siRNA (Ganem and Compton, 2004), which are consistent with the antibody inhibiting Kif2a function in *Xenopus* egg extracts.

Addition of Kif2a antibody (0.7 mg/ml) to assembled bipolar spindles resulted in an increase in spindle microtubule length, evident from buckled and wavy microtubule bundles

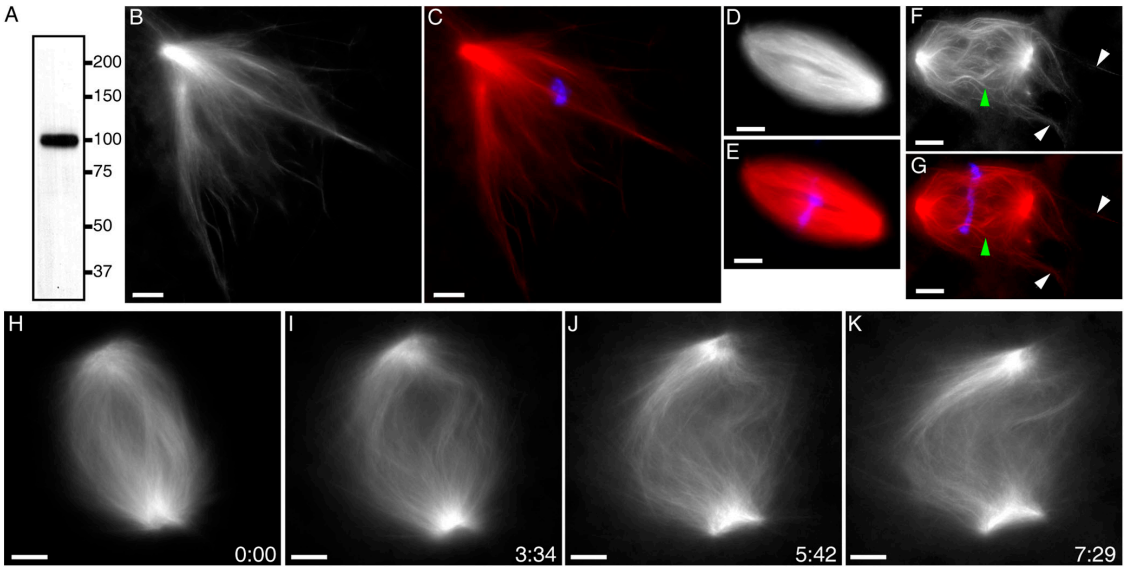

Figure 4. **Kif2a is required for bipolar spindle assembly and the regulation of spindle microtubule length.** (A) Western blot of *Xenopus* egg extracts stained with anti-Kif2a. Molecular weight standards are shown. (B–E) Anti-Kif2a inhibits bipolar spindle assembly. Anti-Kif2a (0.7 mg/ml; B and C) or control buffer (D and E) were added at the start of assembly reactions. (B and D) Tubulin alone. (C and E) Overlay (tubulin, red; DNA, blue). (F–K) Anti-Kif2a (0.7 mg/ml) was added to assembled spindles. (F and G) 8 min after antibody addition. Long microtubule bundles extended beyond (white arrowheads), and buckled (green arrowheads) within the spindle. (F) Tubulin alone. (G) Overlay (tubulin, red; DNA, blue). (H–K) Real-time analysis of a spindle treated with anti-Kif2a (added ~3 min before image at t = 0; Video 6). Times are in min:s. Bars, 10 μm.

in spindles (Fig. 4, F and G, green arrowheads), and also from long microtubules extending out from spindles (Fig. 4, F and G, white arrowheads). However, the pole to pole distance did not increase to accommodate these increases in microtubule length. Real-time analysis also revealed increases in microtubule length that did not result in corresponding increases in spindle length (Fig. 4, H–K; Video 6, available at http://www.jcb.org/cgi/content/full/jcb.200404015/DC1). At ~20 min after antibody addition, spindles often became highly disorganized and lost bipolar organization. Due to continuous changes in microtubule curvature, and complex trajectories of spindle pole movements (in 3-dimensions), we were unable to quantitatively analyze microtubule dynamics upon Kif2a inhibition. However, similar to the consequences of inhibiting dynein, dynactin, or NuMA, Kif2a inhibition increased the lengths of spindle microtubules.

Dynein/dynactin and NuMA are required for the targeting of Kif2a to spindle poles

To test whether increases in spindle microtubule length upon dynein, dynactin, or NuMA inhibition were due to perturbation of KinI activities at spindle poles, we examined the localization of Kif2a and MCAK in spindles treated with p150-CC1 or antibody 70.1. In control samples, we found that MCAK targeted to spindle poles, which is consistent with previous reports (Fig. 5, A, D, and G; Walczak et al., 1996). Under these fixation conditions we found that Kif2a also localized to spindle poles (Fig. 5, J, M, and P). In elongating spindles treated with p150-CC1 or 70.1, MCAK targeted to spindle poles, and its distribution, relative to microtubules, was not significantly perturbed (Fig. 5, A– I). The accumulation of Kif2a at spindle poles in the presence of p150-CC1 or 70.1 was diminished (Fig. 5, J–R). LGN-N treated spindles also revealed that Kif2a, but not MCAK, targeting was perturbed (not depicted). Spindles fixed using different conditions (methanol instead of formaldehyde) revealed that Kif2a, like MCAK, also targeted to sites of chromosome-microtubules attachment, which is consistent with these proteins targeting to kinetochores (Fig. S3, available at http://www.jcb.org/cgi/content/full/jcb.200404015/DC1). Treatment with p150-CC1 did not disrupt the targeting of Kif2a to kinetochores. As another measure of the dependence on dynactin of KinI targeting to spindles, we partially purified spindles by pelleting through a glycerol cushion, and determined the amounts of spindle-associated MCAK and Kif2a by immunoblotting. Using this assay, we also found that dynactin inhibition reduced the amount of spindle-associated Kif2a, but not MCAK, relative to tubulin (Fig. 5, S–U). Although we are unable to detect a direct interaction between NuMA or dynein/dynactin and Kif2a using available reagents, our data are consistent with dynactin and NuMA targeting, or maintaining, Kif2a at spindle poles.

It is possible that Kif2a is the functional homologue of Klp10, the *Drosophila* KinI motor (Goshima and Vale, 2003), and its effect on microtubule dynamics may be specific to spindle poles (Rogers et al., 2004). Our works demonstrate that Kif2a plays an important role in regulating the length of spindle microtubules, but do not confirm its site-specific activity. We propose that dynein, dynactin, and NuMA regulate spindle microtubule length by localizing the depolymerizing activity of Kif2a to spindles poles. Our work also reveals that NuMA and dynein/dynactin play a role in maintaining a mechanical constraint that keeps spindle poles from separating, even when spindle microtubules get unusu-

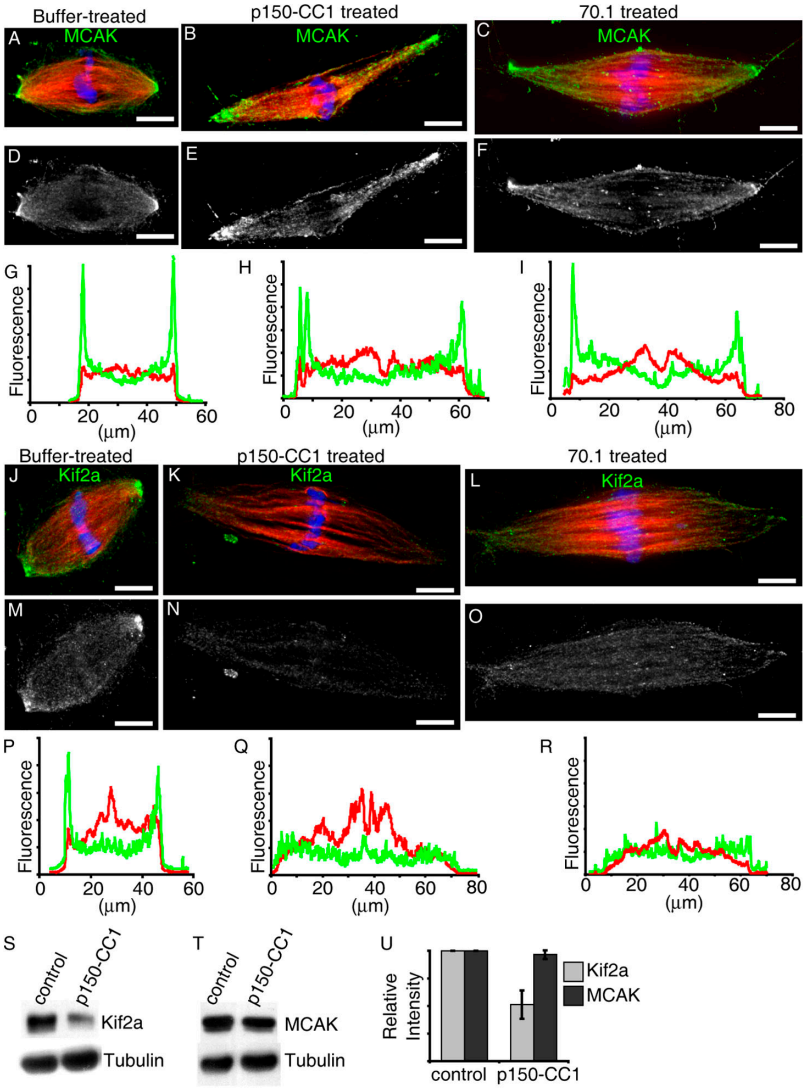

Figure 5. **Treatment with p150-CC1 or 70.1 displaces Kif2a, but not MCAK from spindle poles.** Assembled spindles, after addition of buffer, p150-CC1, or 70.1, were processed for immunofluorescence. MCAK staining in control (A and D), p150-CC1–treated (2 μM, 15 min; B and E), and 70.1-treated (1 mg/ml, 15 min; C and F) spindles. (A–C) Overlays (tubulin, red; DNA, blue; MCAK, green). (D–F) MCAK alone. (G–I) Line scans of fluorescence intensity (MCAK, green; tubulin, red; arbitrary units) across the pole to pole axis of the spindles shown in A–C. Kif2a staining in untreated (J and M), p150-CC1–treated (2 μM, 15 min; K and N), and 70.1-treated (1 mg/ml, 15 min; L and O) spindles. (J–L) Overlays (tubulin, red; DNA, blue; Kif2a, green). (M–O) Kif2a alone. (P–R) Line scans of fluorescence intensity (Kif2a, green; tubulin, red; arbitrary units) across the pole to pole axis of the spindles shown in (J–L). (S and T) Spindles were treated for 15 min with p150-CC1 (4 μM) or control buffer and the relative amount of Kif2a (S), or MCAK (T), and tubulin associated with partially purified spindle pellets was analyzed by immunoblotting. (U) Quantitation of spindle-associated Kif2a and MCAK relative to tubulin from measurements of immunoblot band intensities (mean ± SD, two independent experiments), normalized to intensities from untreated spindles. Bars, 10 μm.

ally long after Kif2a inhibition. Our data also provide insight into mechanisms of polewards flux. The fact that microtubule assembly/disassembly can do mechanical work, has been demonstrated in vitro and in the context of spindles (Lombillo et al., 1995; Waters et al., 1996; Fygenson et al., 1997). This raises the possibility that the force driving flux could come from microtubule disassembly at poles. Microtubules could be "reeled in" from poles without a separate force-generating component driving microtubule sliding. Our data show that microtubule disassembly can be suppressed without affecting the rates of microtubule translocation in spindles. Therefore, the disassembly of microtubules is not required for the force generating mechanism driving polewards flux and this force is more likely to be produced by the sliding mechanism. Furthermore, this sliding mechanism does not involve dynein/dynactin or NuMA.

Materials and methods

Reagents

Spindles were assembled in cytostatic factor–arrested *Xenopus laevis* extracts cycled once though interphase to replicate DNA and centrosomes as described previously (Desai et al., 1999a). Tubulins labeled with fluorophores (Hyman et al., 1991), and p50 dynamitin (Wittmann and Hyman, 1999) were prepared as described previously. p150-CC1 was expressed and purified as described previously (King et al., 2003), and dialyzed into buffer XB1 (10 mM Hepes, 150 mM sucrose, 250 mM KCl, 1 mM $MgCl_2$, 1 mM DTT plus protease inhibitors). Expression construct was a gift from T. Schroer (Johns Hopkins University, Baltimore, MD). LGN-N fused to GST was expressed in *E. coli* BL21(DE3) from the pGEX2T vector (Amersham Biosciences), purified on a glutathione-agarose column (Sigma-Aldrich), and dialyzed into buffer XB1. Expression construct was a gift from I. Macara (University of Virginia, Charlottesville, VA). Dynein intermediate chain antibody 70.1 (Sigma-Aldrich) was prepared as described previously (Heald et al., 1996), and used at 1:10 dilution. Polyclonal rabbit anti-Kif2a was a gift from D.A. Compton (Dartmouth Medical School, Hanover, NH).

Immunofluorescence and microscopy

Samples for immunofluorescence were fixed in 2% formaldehyde processed for immunofluorescence as described previously (Desai et al., 1999a). Anti-Kif2a was used at 1 μg/ml and anti–α-tubulin (clone DM1a; Sigma-Aldrich) was used at 1:3,000 dilution. Images were acquired as 3-D volumes using a DeltaVision system (Applied Precision Instruments) and processed using iterative constrained deconvolution.

Fluorescence imaging of spindles in extract was done using an Axiovert 200M (Carl Zeiss MicroImaging, Inc.) with either a 40× (Plan Neo, NA 0.75, for tracking spindle length) or 63× (Plan Apo, NA 1.4, for fluorescence speckle microscopy and imaging microtubule organization) objective. An Orca ER CCD camera (Hamamatsu) was used. Fluorophore-conjugated tubulins were used for fluorescent speckle microscopy at ~11 nM (X-rhodamine) and for visualizing microtubule organization at ~300 nM

(X-rhodamine or Alexa-488). For fluorescent speckle microscopy, 350–500-msec exposures were acquired at 2–5-s intervals. All real-time imaging experiments were performed at 18°C.

Spindle pelleting

Extract samples were diluted 1:10 in BRB80, 30% glycerol, 0.5% Triton X-100, overlaid on 1-ml cushion (BRB80, 40% glycerol), and centrifuged for 15 min at 6,000 *g*. Spindle pellets were resuspended in 1-ml cushion and recentrifuged for 15 min at 6,000 *g*. The final spindle pellet was analyzed by immunoblotting. KinI and tubulin band intensities were recorded by scanning (HP scanjet 5470c), and quantified using Metamorph software.

Data analysis

Analysis was performed using Metamorph software (Universal Imaging Corp.). The length of a line drawn from one spindle pole to the other was used to measure spindle length. Kymographs were prepared from unprocessed images by selecting the maximum intensity across a 7-pixel-wide (x dimension) region aligned with the spindle axis (y dimension). Slopes of fluorescent speckle streaks in the kymographs were measured to calculate speckle velocity. Line scans were generated from the average intensity across a 10-pixel-wide line across the image.

Online supplemental material

Online supplemental material includes: (a) methods for immunofluorescence to examine kinetochore localization of Kif2a; (b) Fig. S1 showing the effect of vanadate on spindle length and comparing the effects of p50 dynamitin and p150-CC1; (c) Fig. S2 showing NuMA localization in spindles treated with p150-CC1 or LGN-N; (d) Fig. S3 showing Kif2a localization at kinetochores; and (e) five videos, corresponding to data in Figs. 1–4. Online supplemental material is available at http://www.jcb.org/cgi/content/full/jcb.200404015/DC1.

We thank Duane Compton for Kif2a antibodies, Trina Schroer (The Johns Hopkins University, Baltimore, MD) for the p150-CC1 expression plasmid, and Ian Macara (University of Virginia, Charlottesville, VA) for the LGN-N construct.

This work was supported by a National Institutes of Health grant (GM65933). T.M. Kapoor is a Pew Scholar. J. Gaetz is an Howard Hughes Medical Institute Predoctoral fellow.

Submitted: 2 April 2004
Accepted: 7 July 2004

References

Cassimeris, L. 1999. Accessory protein regulation of microtubule dynamics throughout the cell cycle. *Curr. Opin. Cell Biol.* 11:134–141.

Desai, A., A. Murray, T.J. Mitchison, and C.E. Walczak. 1999a. The use of *Xenopus* egg extracts to study mitotic spindle assembly and function in vitro. *Methods Cell Biol.* 61:385–412.

Desai, A., S. Verma, T.J. Mitchison, and C.E. Walczak. 1999b. Kin I kinesins are microtubule-destabilizing enzymes. *Cell.* 96:69–78.

Du, Q., P.T. Stukenberg, and I.G. Macara. 2001. A mammalian partner of inscuteable binds NuMA and regulates mitotic spindle organization. *Nat. Cell Biol.* 3:1069–1075.

Du, Q., L. Taylor, D.A. Compton, and I.G. Macara. 2002. LGN blocks the ability of NuMA to bind and stabilize microtubules. A mechanism for mitotic spindle assembly regulation. *Curr. Biol.* 12:1928–1933.

Echeverri, C.J., B.M. Paschal, K.T. Vaughan, and R.B. Vallee. 1996. Molecular characterization of the 50-kD subunit of dynactin reveals function for the complex in chromosome alignment and spindle organization during mitosis. *J. Cell Biol.* 132:617–633.

Fygenson, D.K., J.F. Marko, and A. Libchaber. 1997. Mechanics of microtubule-based membrane extension. *Phys. Rev. Lett.* 79:4497–4500.

Ganem, N., and D.A. Compton. 2004 The KinI kinesin Kif2a is required for bipolar spindle assembly through a functional relationship with MCAK. *J. Cell Biol.* 166:473–478.

Gaglio, T., A. Saredi, and D.A. Compton. 1995. NuMA is required for the organization of microtubules into aster-like mitotic arrays. *J. Cell Biol.* 131:693–708.

Goshima, G., and R.D. Vale. 2003. The roles of microtubule-based motor proteins in mitosis: comprehensive RNAi analysis in the *Drosophila* S2 cell line. *J. Cell Biol.* 162:1003–1016.

Heald, R., R. Tournebize, T. Blank, R. Sandaltzopoulos, P. Becker, A. Hyman, and E. Karsenti. 1996. Self-organization of microtubules into bipolar spindles around artificial chromosomes in *Xenopus* egg extracts. *Nature.* 382: 420–425.

Heald, R., R. Tournebize, A. Habermann, E. Karsenti, and A. Hyman. 1997. Spindle assembly in *Xenopus* egg extracts: respective roles of centrosomes and microtubule self-organization. *J. Cell Biol.* 138:615–628.

Howell, B.J., B.F. McEwen, J.C. Canman, D.B. Hoffman, E.M. Farrar, C.L. Rieder, and E.D. Salmon. 2001. Cytoplasmic dynein/dynactin drives kinetochore protein transport to the spindle poles and has a role in mitotic spindle checkpoint inactivation. *J. Cell Biol.* 155:1159–1172.

Hyman, A., D. Drechsel, D. Kellogg, S. Salser, K. Sawin, P. Steffen, L. Wordeman, and T. Mitchison. 1991. Preparation of modified tubulins. *Methods Enzymol.* 196:478–485.

Karki, S., and E.L. Holzbaur. 1999. Cytoplasmic dynein and dynactin in cell division and intracellular transport. *Curr. Opin. Cell Biol.* 11:45–53.

King, S.J., C.L. Brown, K.C. Maier, N.J. Quintyne, and T.A. Schroer. 2003. Analysis of the dynein-dynactin interaction in vitro and in vivo. *Mol. Biol. Cell.* 14:5089–5097.

Lombillo, V.A., R.J. Stewart, and J.R. McIntosh. 1995. Minus-end-directed motion of kinesin-coated microspheres driven by microtubule depolymerization. *Nature.* 373:161–164.

Maddox, P., A. Desai, K. Oegema, T.J. Mitchison, and E.D. Salmon. 2002. Poleward microtubule flux is a major component of spindle dynamics and anaphase a in mitotic *Drosophila* embryos. *Curr. Biol.* 12:1670–1674.

Merdes, A., K. Ramyar, J.D. Vechio, and D.W. Cleveland. 1996. A complex of NuMA and cytoplasmic dynein is essential for mitotic spindle assembly. *Cell.* 87:447–458.

Merdes, A., R. Heald, K. Samejima, W.C. Earnshaw, and D.W. Cleveland. 2000. Formation of spindle poles by dynein/dynactin-dependent transport of NuMA. *J. Cell Biol.* 149:851–862.

Mitchison, T.J. 1989. Polewards microtubule flux in the mitotic spindle: evidence from photoactivation of fluorescence. *J. Cell Biol.* 109:637–652.

Noda, Y., R. Sato-Yoshitake, S. Kondo, M. Nangaku, and N. Hirokawa. 1995. KIF2 is a new microtubule-based anterograde motor that transports membranous organelles distinct from those carried by kinesin heavy chain or KIF3A/B. *J. Cell Biol.* 129:157–167.

Quintyne, N.J., S.R. Gill, D.M. Eckley, C.L. Crego, D.A. Compton, and T.A. Schroer. 1999. Dynactin is required for microtubule anchoring at centrosomes. *J. Cell Biol.* 147:321–334.

Rogers, G.C., S.L. Rogers, T.A. Schwimmer, S.C. Ems-McClung, C.E. Walczak, R.D. Vale, J.M. Scholey, and D.J. Sharp. 2004. Two mitotic kinesins cooperate to drive sister chromatid separation during anaphase. *Nature.* 427:364–370.

Walczak, C.E., T.J. Mitchison, and A. Desai. 1996. XKCM1: a *Xenopus* kinesin-related protein that regulates microtubule dynamics during mitotic spindle assembly. *Cell.* 84:37–47.

Walczak, C.E., E.C. Gan, A. Desai, T.J. Mitchison, and S.L. Kline-Smith. 2002. The microtubule-destabilizing kinesin XKCM1 is required for chromosome positioning during spindle assembly. *Curr. Biol.* 12:1885–1889.

Waterman-Storer, C.M., A. Desai, J.C. Bulinski, and E.D. Salmon. 1998. Fluorescent speckle microscopy, a method to visualize the dynamics of protein assemblies in living cells. *Curr. Biol.* 8:1227–1230.

Waters, J.C., T.J. Mitchison, C.L. Rieder, and E.D. Salmon. 1996. The kinetochore microtubule minus-end disassembly associated with poleward flux produces a force that can do work. *Mol. Biol. Cell.* 7:1547–1558.

Wittmann, T., and T. Hyman. 1999. Recombinant p50/dynamitin as a tool to examine the role of dynactin in intracellular processes. *Methods Cell Biol.* 61: 137–143.

Wittmann, T., A. Hyman, and A. Desai. 2001. The spindle: a dynamic assembly of microtubules and motors. *Nat. Cell Biol.* 3:E28–E34.

Yu, F., X. Morin, Y. Cai, X. Yang, and W. Chia. 2000. Analysis of partner of inscuteable, a novel player of *Drosophila* asymmetric divisions, reveals two distinct steps in inscuteable apical localization. *Cell.* 100:399–409.